

Observation of the Bloch-Siegert shift in the driven quantum-to-classical transition of a dispersive transmon qubit

I. Pietikäinen¹, S. Danilin², K. S. Kumar², D. S. Golubev², J. Tuorila^{1,3}, and G. S. Paraoanu²

¹*Department of Physics, University of Oulu, P.O. Box 3000, FI-90014, Finland*

²*Centre for Quantum Engineering and LTQ, Department of Applied Physics, Aalto University, P.O. Box 15100, FI-00076 Aalto, Finland and*

³*COMP Centre of Excellence, Department of Applied Physics, Aalto University, P.O. Box 15100, FI-00076 Aalto, Finland*

(Dated: November 7, 2022)

We demonstrate the Bloch-Siegert effect in a dispersively coupled qubit-cavity system which is driven through a quantum-to-classical transition. The observed dispersive shift of the resonance frequency displays strongly non-monotonic dependence on the number of cavity photons and escapes the scope of the analytic results obtained with either a simple rotating-wave approximation, or with a more refined counter-rotating hybridized rotating wave approach. We measured the transition energy with a weak resonant probe, and the obtained data is in a good agreement with our numerical simulations of the quasienergy spectrum.

The energy levels of a quantum system change by coupling to a coherently driven radiation field. This is called the dynamic (ac) Stark effect. A paradigmatic example is the spin- $\frac{1}{2}$ particle driven by a transversely polarized radio-frequency field [1]. In the rotating wave approximation (RWA), the results align with those of a simpler circular polarization. When the drive amplitude becomes a considerable fraction of spin's Larmor frequency, the RWA results have to be corrected by inclusion of the counter-rotating field terms, resulting in the Bloch-Siegert (BS) shift of the transition energy [2]. Bloch-Siegert effects are relevant for a variety of phenomena and experimental platforms, including spins [3, 4], atomic systems [5], and with superconducting qubits with vacuum [6] and strongly driven [7] fields.

When a superconducting transmon qubit is placed inside a co-planar waveguide resonator, acting as a microwave cavity, one obtains a circuit which can mimic the behaviour of cavity quantum electrodynamics (QED) [8]. Due to the analogy, such systems are referred to as circuit QED. Coupling between the qubit and the cavity leads to hybridization of their respective bare frequencies ω_0 and ω_c . When the coupling is bilinear and weak, the system can be modelled with the Jaynes-Cummings (JC) Hamiltonian, characterized by the strength g of the coupling. Especially, when the qubit and the cavity are detuned ($|\omega_0 - \omega_c| \gg g$), the cavity frequency ω_c experiences the dispersive shift $\chi_0 = g^2/|\omega_0 - \omega_c|$ whose sign is different for the two qubit states (Fig. 1). Strong transverse driving [9] or an increase in the temperature [10] saturate the qubit and, as a consequence, the dispersive shift of the cavity becomes averaged out in a process which is analogous to motional averaging [3, 11]. This can also be seen as emergence of classical physics from the inherent quantum behaviour [10, 12]. Similar renormalization effect of the cavity frequency is also present when the cavity is driven, which has been used in high-fidelity single-shot measurements of the qubit state [13–15].

In this letter, we study the changes in the probe resonance frequency of a circuit QED system caused by the interplay between the dispersive coupling and an intensity-controlled harmonic cavity drive. We explain the resulting renormalization of the resonance frequency as the transition from quantum to classical behaviour of the system. We show that the renormalization displays non-monotonic dependence on the number of photons in the cavity and escapes the scope of the simple RWA, and

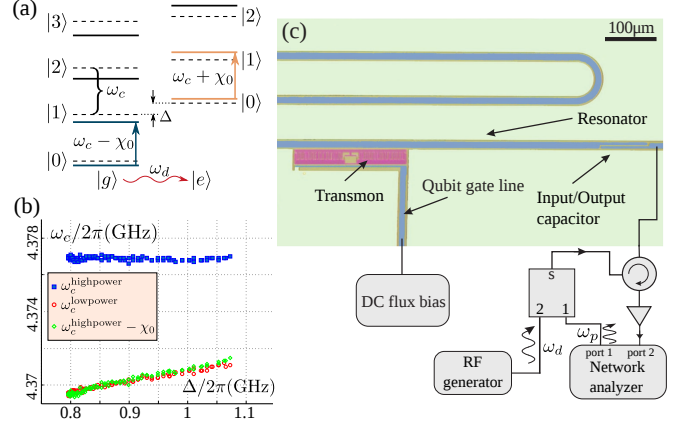


FIG. 1: Schematic of the experimental setup. (a) Energy levels of a dispersive JC system. The diagonalized system is composed of two independent non-linear oscillators, one for each qubit state $|g\rangle$ and $|e\rangle$. The qubit occupation can be changed by tuning the intensity of the drive tone ω_d , and the measured weak cavity probe spectrum $S(\omega_p)$ is obtained as the qubit occupation weighted average of the two oscillator spectra (blue and orange). (b) Cavity resonance frequency at high (blue) and low (red) drive powers as a function of the qubit cavity detuning $\Delta = \omega_0 - \omega_c$. Fit with the theoretical dispersive shift (green) shows that the saturation effect is independent on the detuning. (c) Optical micrograph of the main elements of the sample (false colors), and a schematic of the room temperature electronics and wiring used in the experiment.

also the more refined counter-rotating hybridized rotating wave (CHRW) approximation [16, 17] for the drive. The measured deviation from the RWA result comprises the first experimental demonstration of the BS effect in a driven quantum-to-classical transition. Due to its weak non-linearity, we have to go beyond the conventional two-state approximation for the transmon in order to quantitatively account for the measured spectrum with a large cavity occupation. Similar physics has also been studied theoretically in the context of dynamic Stark effect in a resonant JC system [18]. Also, the energy levels and coherent destruction of tunnelling in a strongly driven qubit-cavity system have been studied in reference [19]. The nonlinear dependence of the cavity occupation on the applied microwave power in a transmon-cavity system has been studied experimentally [20]. Our measurement represents a step towards experimental studies of quantum-to-classical phase transitions [21, 22] and novel quantum simulations in interacting photonic lattices [23, 24] in one-dimensional circuit QED lattices [25].

Our system consists of a superconducting transmon qubit coupled capacitively to a quarter-wave coplanar waveguide resonator, which acts as a microwave cavity with the bare resonance frequency ω_c (Fig. 1). The qubit is realized as a split-Cooper pair box operated at the transmon limit [8]. Its transition frequency ω_0 can be controlled with external magnetic flux flowing through its superconducting loop. The cavity is excited by a microwave tone ω_d , which allows us to study a broad range of the average cavity occupation (up to ~ 10000 photons). We investigate the combined effect of strong driving and the qubit-cavity coupling g on the cavity frequency by measuring the reflection coefficient $\Gamma(\omega_p)$ of an additional small-amplitude microwave probe tone ω_p whose frequency is swept in a range of a few tens of MHz around the bare resonant frequency of the cavity. It should be emphasized that we are probing the effective steady state cavity frequency, instead of the transient cavity response which reveals the initial qubit state [13–15].

Theory – The transmon is essentially a weakly nonlinear multi-level system. In the following considerations, we take into account only the two lowest energy levels. A more quantitative comparison with the experiments is made with numerical simulations including up to seven transmon states.

In the frame where the driven cavity is displaced into the vacuum [26], the Hamiltonian of our cavity-driven two-state transmon can be written as (energies scaled with \hbar)

$$\hat{H} = \omega_c \hat{a}^\dagger \hat{a} + \frac{\omega_0}{2} \hat{\sigma}_z + g(\hat{a}^\dagger + \hat{a}) \hat{\sigma}_x + G \cos(\omega_d t) \hat{\sigma}_x, \quad (1)$$

where \hat{a} is the annihilation operator of the cavity, and $\hat{\sigma}_i$, $i = x, y, z$, are the Pauli spin matrices. Also, $G = gA/\sqrt{\delta_c^2 + \kappa^2/4}$ is the effective qubit drive amplitude, where A is the amplitude of the cavity drive, $\delta_c \equiv \omega_c - \omega_d$

is detuning between the cavity and the drive, and κ is the cavity dissipation. To obtain a simple and intuitive picture of the relevant physics, we make RWAs for the cavity-qubit coupling and for the drive. Notice that the RWA made for the cavity-qubit coupling accounts for the JC approximation in the displaced frame. However, we expect that our RWA for the drive becomes insufficient as G diverges with increasing microwave amplitude A . In the dispersive limit, the static JC Hamiltonian can be diagonalized with a Schrieffer-Wolff transformation $\hat{U} = \exp[-\frac{g}{\omega_0 - \omega_c}(\hat{a}\hat{\sigma}_+ - \hat{a}^\dagger\hat{\sigma}_-)]$, where $\hat{\sigma}_-$ is the annihilation operator of the qubit. By taking into account terms up to second order in g , we obtain

$$\hat{H} = (\omega_c + \chi_0 \hat{\sigma}_z) \hat{a}^\dagger \hat{a} + \frac{1}{2}(\omega_0 + \chi_0) \hat{\sigma}_z + \frac{G}{2} (e^{i\omega_d t} \hat{\sigma}_- + e^{-i\omega_d t} \hat{\sigma}_+). \quad (2)$$

We have neglected non-linear coupling terms and a cavity driving term, leading into decoupling of the cavity and the drive. Thus, we see that the above Hamiltonian is formed by a driven qubit and two oscillators with frequencies $\omega_c \pm \chi_0$, where $-(+)$ stands for the ground (excited) state of the qubit. Since the oscillators are independent, transitions between states of different oscillators cannot be induced with a cavity probe. As a consequence, the probe spectrum is formed by a weighted average of the oscillator spectra (see Fig. 1(a)).

By writing the cavity part of Hamiltonian (2) in the semi-classical approximation ($\hat{\sigma}_z \hat{a}^\dagger \hat{a} \approx \langle \hat{\sigma}_z \rangle \hat{a}^\dagger \hat{a}$), we obtain

$$\hat{H} = (\omega_c + \chi_0 \langle \hat{\sigma}_z \rangle) \hat{a}^\dagger \hat{a}, \quad (3)$$

where the steady state population of the qubit $\langle \hat{\sigma}_z \rangle = -\delta_q^2/(\delta_q^2 + G^2/2)$ and $\delta_q \equiv \omega_0 - \omega_d$ is the detuning between the qubit and the drive. Thus, we can say that the cavity frequency is renormalized by the qubit-state which can be tuned with the drive as the flipping frequency G increases with amplitude A . In the frame where the qubit-cavity interaction is diagonalized, the cavity frequency is shifted from $\omega_c - \chi_0 \rightarrow \omega_c$ due to the saturation of the transversely driven qubit with increasing microwave power. This is a coherent equivalent of the motional averaging effect observed with spin- $\frac{1}{2}$ particles in a discretely varying magnetic environment [3].

Since G diverges with increasing A , we expect that the RWA becomes insufficient at large drive powers. On the other hand, it is well known [27] that the RWA is basis-dependent. So, instead of making the RWA in the laboratory frame of the qubit, we first make a unitary transformation $\hat{U} = \exp[-i(G/\omega_d)\xi \sin(\omega_d t)\hat{\sigma}_x]$, where ξ is determined from the equation $G/2 \equiv G(1 - \xi) = \omega_0 J_1(2G\xi/\omega_d)$ [26]. By neglecting the second and higher order harmonics of ω_d , one can write the total Hamilto-

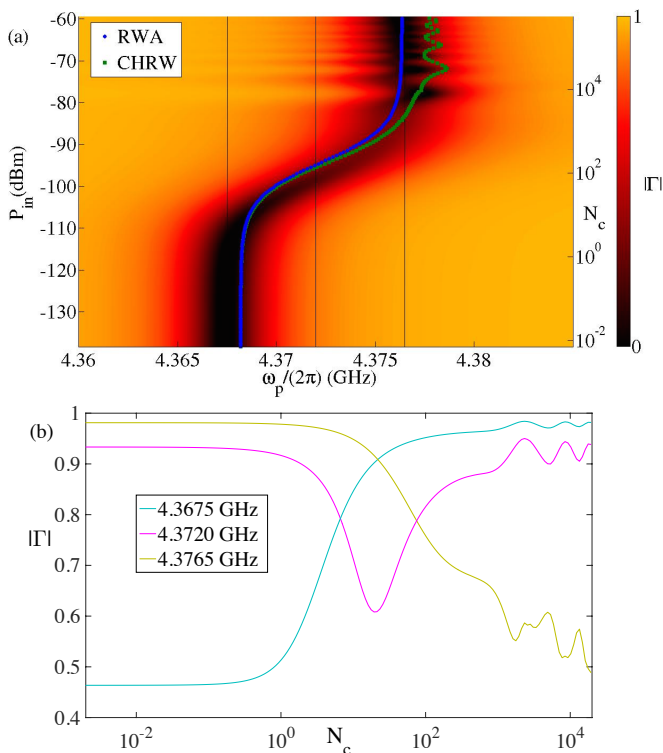


FIG. 2: Renormalization and Bloch-Siegert shift of the resonance frequency of system formed by coupled cavity and a two-level transmon. We use the experimental values for the natural frequencies $\omega_c/(2\pi) = 4.376$ GHz, $\omega_0/(2\pi) = 5.16$ GHz, and $g/(2\pi) = 80$ MHz. (a) Probe reflection coefficient $|\Gamma|$ as a function of probe frequency ω_p and cavity occupation N_c . The dark tone indicates strong absorption from the probe. The theoretical curves are produced with the RWA (blue) and CHRW (green) approximations. (b) Reflection coefficients for three different probe frequencies indicated with dashed vertical lines in (a).

nian as

$$\hat{H} = \omega_c \hat{a}^\dagger \hat{a} + \frac{\tilde{\omega}_0}{2} \hat{\sigma}_z + g(\hat{a}^\dagger + \hat{a})\hat{\sigma}_x + \frac{\tilde{G}}{2}(e^{i\omega_d t} \hat{\sigma}_- + \text{h.c.}), \quad (4)$$

where h.c. stands for hermitian conjugate. We see that this is formally equal to (1) with RWA on the drive term. However, also the qubit energy $\tilde{\omega}_0 \equiv \omega_0 J_0(2G\xi/\omega_d)$ and the amplitude \tilde{G} are renormalized by the strong drive. We have denoted the Bessel functions of the first kind with J_m . The above CHRW Hamiltonian [16, 17] results in dynamics that have been proven very accurate when compared to full numerical solutions with $G/\omega_d < 1$ and even for higher values of G when $\omega_0/\omega_d < 1$ [16]. However, here we are interested in broad range of G for $\omega_0 > \omega_d$ and, thus, we expect that the contributions arising from the second and higher harmonics, neglected in the above discussion, become notable.

We plot in Fig. 2 the renormalized resonance frequencies in the RWA and CHRW approximations. We compare the results with the numerical simulations of the re-

flexion coefficient $\Gamma(\omega_p) = (Z(\omega_p) - Z_0)/(Z(\omega_p) + Z_0)$, where $Z(\omega_p)$ and Z_0 are the impedances of the driven cavity coupled to a two-level transmon and the transmission line, respectively. The impedance $Z(\omega_p)$ was calculated from the probe induced transition rates between the quasienergy states [28] of the driven cavity-transmon system by employing the Kramers-Kronig relation [26, 29–31]. We see that the RWA gives the overall qualitative behaviour relatively well but lacks the non-monotonic behaviour of the simulated resonance frequency toward the high power end of the spectrum. On the other hand, the CHRW approximation is non-monotonic but fails to match quantitatively with the average numerical resonance at high drive powers, since it neglects the second and higher harmonics of the drive. Also, with intermediate drive powers, the renormalized qubit becomes resonant with the cavity and the dispersive approximation is not valid. We thus conclude that the deviations from the RWA result at high powers are caused by the counter-rotating drive terms and can, thus, be seen as a characteristic of the Bloch-Siegert effect. Also, in the CHRW approach, full agreement with the numerical results would require the inclusion of higher harmonics, resulting in the generalized BS effect in the CHRW frame [7].

Fig. 2(b) predicts the existence of three regimes: at small average photon numbers, the response of the system is fully quantum mechanical and corresponds to an ac-Stark shifted cavity. When the number of photons becomes of the order of unity, the response is sensitive to the addition or removal of photons, indicating photon blockade. At large number of photons, the spectrum is saturated and the Bloch-Siegert shift produces an oscillatory response as a function of added photons. We demonstrate also that in this region of high intensity the higher energy levels of the transmon become excited, completing the transition to classical regime.

Experimental results – Our experimental sample shown in Fig. 1 is a coplanar superconducting structure made of thin (90 nm) aluminum film deposited on the surface of a pure silicon substrate. The structure consists of a $\lambda/4$ waveguide resonator cavity which is capacitively coupled to a transmon qubit with $E_J^{\text{max}}/E_C = 58$. The bare resonance frequency of the cavity is $\omega_c/(2\pi) = 4.376$ GHz. The energy spectrum of the transmon can be tuned by changing the dc current flowing in the qubit gate line electrode. In our measurements of the cavity renormalization, we fixed the qubit energy to $\omega_0/(2\pi) = 5.16$ GHz. The sample was placed at the mixing chamber plate of a dilution refrigerator, whose temperature was in the range of 20 ~ 25 mK during the measurements.

In the experiment, we combined the two microwave tones, ω_d and ω_p , at room temperature and sent them to the cavity through an input/output capacitor. The drive tone with the frequency ω_d was used to control the average photon number in the cavity. The other microwave tone ω_p was used as a probe of the resonance frequency

of the cavity. The reflected part of the cavity signal was amplified and then recorded by the vector network analyzer, resulting in the reflection coefficient $\Gamma = S_{21}$. The probe tone ω_p was swept in a ~ 40 MHz range around the bare cavity frequency in order to observe any changes in the location of the resonance as the cavity occupation was varied.

In Fig. 3, we show the measured reflection coefficient Γ as a function of the probe frequency ω_p and the number of cavity quanta N_c at the off-resonant drive frequency $\omega_d/(2\pi) = 4.35$ GHz. The three regimes of ac-Stark shift, photon blockade, and BS effect are clearly visible in the experimental data. By comparing the experimental data with the numerical simulation of the reflection coefficient, we see that the simple two-state approximation for the transmon is inadequate to reproduce the location of the measured renormalized cavity frequency in photon blockade and BS parts ($N_c > 1$) of the spectrum. We also note that at the low-power part of the spectrum, the vacuum BS shift is displayed as the difference between the RWA and experimental resonances.

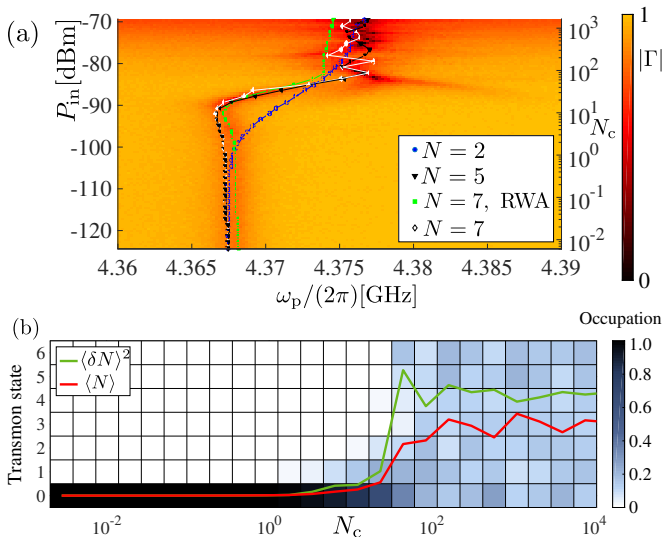


FIG. 3: Demonstration of the resonance frequency renormalization and Bloch-Siegert effect in a coupled transmon-cavity system. (a) The reflection coefficient $|\Gamma|$ as a function of the probe frequency ω_p and the input power P_{in} at the sample (or average number of cavity quanta N_c in the laboratory frame; calibration presented in Supplemental material [26]). Dark tone indicates large absorption from the probe. The drive frequency is $\omega_d/(2\pi) = 4.35$ GHz. Other parameters are the same as in Fig. 2. The numerical data has converged up to $N_c \approx 100$ for $N = 7$. (b) Occupation of the transmon states as a function of cavity occupation.

In the displaced frame, the cavity drive is transformed into a transmon drive. Since the transmon is only weakly non-linear, the strong driving causes excitation to higher transmon states. The data shows that the inclusion of the counter-rotating drive terms and transmon states more

than $N = 7$ are needed to have a quantitative agreement with our high-power data. In Fig. 3(b), we also demonstrate that the fluctuations $\langle \delta N \rangle^2 = \langle N^2 \rangle - \langle N \rangle^2$ of the transmon occupation number change rather abruptly when the drive power is swept over the transition regime between the ac-Stark and saturated part of the spectrum. We interpret these as an indication of a phase transition between the quantum and the classical regimes of the combined qubit-resonator system [21]. In the quantum regime, the transmon behaves as a two-level system (qubit) with only σ_z -coupling to the resonator. In consequence, the two systems can be addressed separately and we can for example perform Rabi oscillations on the qubit and use the resonator for readout. In the classical regime, this is no longer possible as the two subsystems become strongly hybridized.

We show in Fig. 3 the numerical data for $q_g = 0$ assuming that there are no stray quasiparticles present in the transmon. For the lowest energy states, the transmon is anyway immune to quasiparticles by design; however, for large- N states the charge insensitivity is no longer guaranteed. For states $N > 7$, the nearly degenerate transmon states are so close that the secular approximation that is made in the derivation of the Floquet-Born-Markov master equation used in our simulations becomes insufficient and causes numerical instabilities.

For the classical part of our experimental spectrum, the transmon states with $N > 6$ are occupied (Fig. 3(b)) and the truncation in the transmon state space has to be done with odd (even) values of N , respectively, so that the nearly degenerate states are properly included.

We have also analyzed the dependence of the classical response as a function of the drive frequency in Fig. 4 and show that the system tends to saturate at the resonant frequency of the bare cavity, with rather small BS oscillations around it irrespective of the value of the drive frequency. Because the transition occurs at fixed value of $N_c \sim 1$ for all drive frequencies [26], we choose to plot the response in fixed interval of cavity quanta ranging from $N_c = 400 \dots 1650$. However, we show in the Supplemental material [26] that the width of the quantum-to-classical transition region broadens when the drive is brought closer to resonance with the cavity. As a consequence, the quantum solution with $N = 5$ matches better with the high-frequency ($\omega_d/(2\pi) = 4.36$ GHz) data whereas for the low-frequency data ($\omega_d/(2\pi) = 4.35$ GHz) the transition has already occurred and system follows the classical resonance location calculated by treating the Josephson junction of the transmon classically and averaging over the drive period [32]. In all plots, we see that power level required for such high values of the cavity occupation result in numerical instabilities that render the $N = 7$ solution inaccurate.

We also did experiments at higher drive frequencies and with different qubit frequencies (see Supplemental material [26]). Qualitatively, the behaviour is similar as

described above. However, when the drive is nearly resonant with the bare cavity, the cavity excites strongly even in the displaced frame and the numerical calculations with our model become intractable due to the necessarily large number of basis states needed for the cavity. It should also be noted that we have modelled the dissipation in the driven Rabi system with coupling to a non-interacting bosonic bath. We assumed Ohmic damping and formed the Floquet-Born-Markov equations in the simple RWA, similar to references [33–35]. However, the resulting transition rates, induced by the coupling to the bath, do not obey detailed balance [36]. This can have notable non-physical effects especially near the quasienergy degeneracies, which can be remedied by applying the second order van Vleck perturbation theory for the driven system, and then making the so-called moderate RWA for the system-bath coupling in the resulting approximate quasienergy eigenbasis [29, 37].

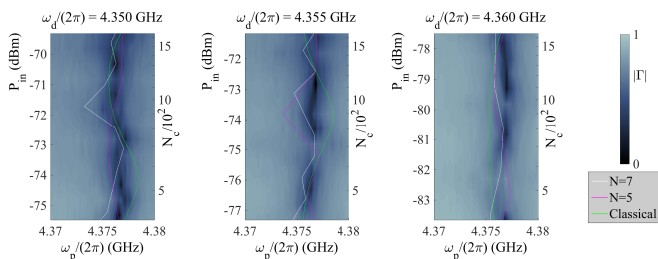


FIG. 4: Magnitude of the Bloch-Siegert effect at high drive powers for drive frequencies $\omega_d/(2\pi) = 4.35, 4.355,$ and 4.36 GHz. We show the experimental contour for the reflection coefficient and compare the resonance location with the classical and numerical results as a function of the probe frequency and fixed range $N_c = 400 \dots 1600$ of the number of cavity quanta.

To conclude, we have studied the circuit QED setup whose cavity is driven strongly. The response of the cavity to a weak probe reveals a Bloch-Siegert shift, which is non-monotonous in the drive power and can be interpreted as the renormalization of the cavity frequency by the transmon occupation. We also showed that by increasing the drive power we were able to excite the transmon from quantum to classical regime. This paves way for future experiments of quantum simulations of dissipative phase transitions in one-dimensional circuit-QED lattices.

Discussions with Erkki Thuneberg, Matti Silveri, and Sami Laine on theory, and Mika Sillanpää and Juha Pirkkalainen on sample design and fabrication are gratefully acknowledged. GSP also thanks D. Angelakis for useful discussions. This work used the cryogenic facilities of the Low Temperature Laboratory/Department of Physics at Aalto University. We are grateful for the financial support from the Academy of Finland (projects No. 263457 and No. 135135), the Magnus Ehrnrooth Foundation, the Finnish Cultural Foundation, FQXi, and the Centres of Excellence ”Low Temperature Quantum Phenomena and Devices” (project No. 250280) and ”Computational Nanoscience” (projects No. 251748 and 284621).

phenomena and Devices” (project No. 250280) and ”Computational Nanoscience” (projects No. 251748 and 284621).

-
- [1] C. Cohen-Tannoudji, J. Dupont-Roc, and G. Grynberg, *Atom-Photon Interactions: Basic Processes and Applications* (Wiley-VCH, Weinheim, 2004).
 - [2] F. Bloch and A. Siegert, *Phys. Rev.* **57**, 522 (1940).
 - [3] A. Abragam, *Principles of Nuclear Magnetism* (Oxford University Press, 1986).
 - [4] C. Cohen-Tannoudji, J. Dupont-Roc, and C. Fabre, *J. Phys. B: Atom. Molec. Phys.* **6**, L218 (1973).
 - [5] D. Fregenal, E. Horsdal-Pedersen, L. B. Madsen, M. Forre, J. P. Hansen, and V. N. Ostrovsky, *Phys. Rev. A* **69**, 031401(R) (2004).
 - [6] P. Forn-Diaz, J. Lisenfeld, D. Marcos, J. J. Garcia-Ripoll, E. Solano, C. J. P. M. Harmans, and J. E. Mooij, *Phys. Rev. Lett.* **105**, 237001 (2010).
 - [7] J. Tuorila, M. Silveri, M. Sillanpää, E. Thuneberg, Yu. Makhlin, and Pertti Hakonen, *Phys. Rev. Lett.* **105**, 257003 (2010).
 - [8] J. Koch, T. M. Yu, J. Gambetta, A. A. Houck, D. I. Schuster, J. Majer, A. Blais, M. H. Devoret, S. M. Girvin, and R. J. Schoelkopf, *Phys. Rev. A* **76**, 042319 (2007).
 - [9] D. I. Schuster, A. Wallraff, A. Blais, L. Frunzio, R.-S. Huang, J. Majer, S. M. Girvin, and R. J. Schoelkopf, *Phys. Rev. Lett.* **94**, 123602 (2005).
 - [10] J. M. Fink, L. Steffen, P. Studer, L. S. Bishop, M. Baur, R. Bianchetti, D. Bozyigit, C. Lang, S. Filipp, P. J. Leek, and A. Wallraff, *Phys. Rev. Lett.* **105**, 163601 (2010).
 - [11] Jian Li, M. P. Silveri, K. S. Kumar, J.-M. Pirkkalainen, A. Vepsäläinen, W. C. Chien, J. Tuorila, M. A. Sillanpää, P. J. Hakonen, E. V. Thuneberg, and G. S. Paraoanu, *Nat. Commun.* **4**, 1420 (2013).
 - [12] M. J. Everitt, W. J. Munro, and T. P. Spiller, *Phys. Rev. A* **79**, 032328 (2009).
 - [13] M. D. Reed, L. DiCarlo, B. R. Johnson, L. Sun, D. I. Schuster, L. Frunzio, and R. J. Schoelkopf, *Phys. Rev. Lett.* **105**, 173601 (2010).
 - [14] M. Boissonneault, J. M. Gambetta, and A. Blais, *Phys. Rev. Lett.* **105**, 100504 (2010).
 - [15] L. S. Bishop, E. Ginossar, and S. M. Girvin, *Phys. Rev. Lett.* **105**, 100505 (2010).
 - [16] Z. G. Lü and H. Zheng, *Phys. Rev. A* **86**, 023831 (2012).
 - [17] Y. Y. Yan, Z. G. Lu, and H. Zheng, *Phys. Rev. A* **91**, 053834 (2015).
 - [18] P. Alsing, D.-S. Guo, and H. J. Carmichael, *Phys. Rev. A* **45**, 5135 (1992).
 - [19] J. Hausinger and M. Grifoni, *Phys. Rev. A* **83**, 030301(R) (2011).
 - [20] B. Suri, Z. K. Keane, L. S. Bishop, S. Novikov, F. C. Wellstood, and B. S. Palmer, *Phys. Rev. A* **92**, 063801 (2015).
 - [21] H. J. Carmichael, *Phys. Rev. X* **5**, 031028 (2015).
 - [22] M.-J. Hwang, R. Puebla, and M. B. Plenio, *Phys. Rev. Lett.* **115**, 180404 (2015).
 - [23] M. J. Hartmann, *J. Opt.* **18**, 104005 (2016).
 - [24] C. Noh and D. G. Angelakis, arXiv:1604.04433 [quant-ph] (2016).
 - [25] M. Fitzpatrick, N. Sundaresan, A. C. Y. Li, J. Koch, and A. A. Houck, arXiv:1607.06895 [cond-mat,

- physics:quant-ph] (2016).
- [26] See supplemental material at xxx.
- [27] M. Silveri, J. Tuorila, M. Sillanpää, E. Thuneberg, Yu. Makhlin, and P. Hakonen, *J. Phys: Conf. Ser.* **400**, 042054 (2012).
- [28] J. H. Shirley, *Phys. Rev.* **138**, B979 (1965); Ya. B. Zeldovich, *ZhETF* **51**, 1492 (1966) [*Sov. Phys. JETP* **24**, 1006 (1967)].
- [29] M. Silveri, J. Tuorila, M. Kemppainen, and E. Thuneberg, *Phys. Rev. B* **87**, 134505 (2013).
- [30] J. Tuorila, M. Silveri, M. Sillanpää, E. Thuneberg, Yu. Makhlin, and P. Hakonen, *Supercond. Sci. Technol.* **26**, 124001 (2013).
- [31] L. D. Landau and E. M. Lifshitz, *Statistical Physics, Part I*, (Oxford: Pergamon, 1980).
- [32] O.-P. Saira, M. Zgirski, K. L. Viisanen, D. S. Golubev, and J. P. Pekola, *Phys. Rev. Applied* **6**, 024005 (2016).
- [33] R. Blümel, R. Graham, L. Sirko, U. Smilansky, H. Walther, and K. Yamada, *Phys. Rev. Lett.* **62**, 341 (1989).
- [34] R. Blümel, A. Buchleitner, R. Graham, L. Sirko, U. Smilansky, and H. Walther, *Phys. Rev. A* **44**, 4521 (1991).
- [35] M. Grifoni and P. Hänggi, *Phys. Rep.* **304**, 229 (1998).
- [36] S. Gasparinetti, P. Solinas, S. Pugnetti, R. Fazio, and J. P. Pekola, *Phys. Rev. Lett.* **110**, 150403 (2013).
- [37] J. Hausinger and M. Grifoni, *Phys. Rev. A* **81**, 022117 (2010).